

Determination of Epithelial Tissue Scattering Coefficient Using Confocal Microscopy

Tom Collier, Dizem Arifler, Anais Malpica, Michele Follen, and Rebecca Richards-Kortum

Abstract—Most models of light propagation through tissue assume the scattering properties of the various tissue layers are the same. The authors present evidence that the scattering coefficient of normal cervical epithelium is significantly lower than values previously reported for bulk epithelial tissue. They estimated the scattering coefficient of normal and precancerous cervical epithelium using measurements of the reflectance as a function of depth from confocal images. Reflectance measurements were taken from *ex vivo* cervical biopsies and fit to an exponential function based upon Beer's law attenuation. The mean scattering coefficients derived were 22 cm^{-1} for normal tissue and 69 cm^{-1} for precancerous tissue. These values are significantly lower than previously reported for bulk epithelial tissues and suggest that scattering of bulk tissue is dominated by the stroma. They also suggest that computational models to describe light propagation in epithelial tissue must incorporate different scattering coefficients for the epithelium and stroma. Further, the lower scattering of the epithelium suggests greater probing depths for fiber optic probes used by optical diagnostic devices which measure reflectance and fluorescence in epithelial tissue. The difference in scattering between normal and precancerous tissue is attributed to increased nuclear size, optical density, and chromatin texture. The scattering coefficients measured here are consistent with predictions of numerical solutions to Maxwell's equations for epithelial cell scattering.

Index Terms—Cervix, confocal microscopy, epithelial tissue, scattering.

I. INTRODUCTION

A NUMBER of optical technologies have recently shown promise for detection of precancerous lesions *in vivo*, including reflectance spectroscopy [1]–[6], fluorescence spectroscopy [7]–[12], Raman spectroscopy [13], [14], confocal imaging [15]–[17], and optical coherence tomography (OCT) [18], [19]. Optical technologies are sensitive to both morphologic architectural and biochemical changes associated with the dysplasia to carcinoma sequence [20], [21]. As precancers develop, the morphology of epithelial cells is altered, with hyperchromasia, pleomorphism, an increased nuclear to cytoplasmic ratio, and increased metabolic activity. Stromal changes also accompany the development of intraepithelial neoplasia,

with increased angiogenesis, decreased matrix density, and other alterations in the epithelial-stromal communication [22]. Recently, a number of studies suggest that optical spectroscopy and imaging can probe changes in both the epithelium and stroma [23]–[25]. As an example, fluorescence spectroscopy has been used to simultaneously probe changes in epithelial metabolism and stromal matrix density [23], [25].

Optical spectroscopy measurements can be made easily *in vivo* using fiber optic-based probes. Several analytic and numeric models have been proposed to mathematically separate the signal recorded from the epithelium and the stroma [23], [25], [26]. Monte Carlo models that simulate the random walk of photons in tissue have been used to suggest creative fiber optic probe designs that can physically separate signal from the epithelium and stroma [27]–[29]. However, in both cases, the accuracy of these models is limited by the relatively incomplete knowledge of the optical properties of each tissue layer. In particular, these models require accurate values for the absorption coefficient, the scattering coefficient, and the scattering anisotropy of both the epithelium and the stroma.

Several methods have been developed to compute the optical properties of tissue from measurements of collimated transmission, diffuse transmission, and diffuse reflectance [30]–[32] or from reflectance measurements made at varying source detector separations [33], [34]. In general, these methods assume that the optical properties of the sample are homogeneous. While optical properties have been derived using these approaches for a number of epithelial tissues, including the bladder, colon, skin, and esophagus [30], [35], [36], it is likely that the reported values are dominated by the optical properties of the stroma, which occupies the largest volume fraction of the tissue and which likely has the largest absorption and scattering coefficients.

In order to use multilayer models of tissue spectroscopy and to design sophisticated fiber optic probes to separate signals from different epithelial and stromal layers, it is critical to have accurate values for the optical properties of the epithelium. Qu and colleagues microdissected the epithelium of bronchial tissue and separately measured scattering of the epithelium and stroma. They measured scattering coefficients of 200 and 225 cm^{-1} at 700 nm for epithelial and stromal tissue, respectively [37]. An alternative to physical sectioning is optical sectioning. Using reflectance-based confocal microscopy, the depth dependence of reflected light from epithelial cells can easily be probed [15]–[17]. Several groups have measured the depth-dependent decay of reflected light in tissue phantoms using both OCT and confocal microscopy; intensity was observed to decay exponentially according to the scattering

Manuscript received November 25, 2002; revised April 21, 2003. This work was supported by the National Institutes of Health under Grant 1 RO1 CA 82880-01.

T. Collier, D. Arifler, and R. Richards-Kortum are with the Departments of Biomedical Engineering and Electrical and Computer Engineering, The University of Texas at Austin, Austin, TX 78712 USA (e-mail: collier@mail.utexas.edu; kortum@mail.utexas.edu).

A. Malpica and M. Follen are with the Departments of Pathology and Gynecologic Oncology, The University of Texas M.D. Anderson Cancer Center, Houston, TX 7730 USA.

Digital Object Identifier 10.1109/JSTQE.2003.814413

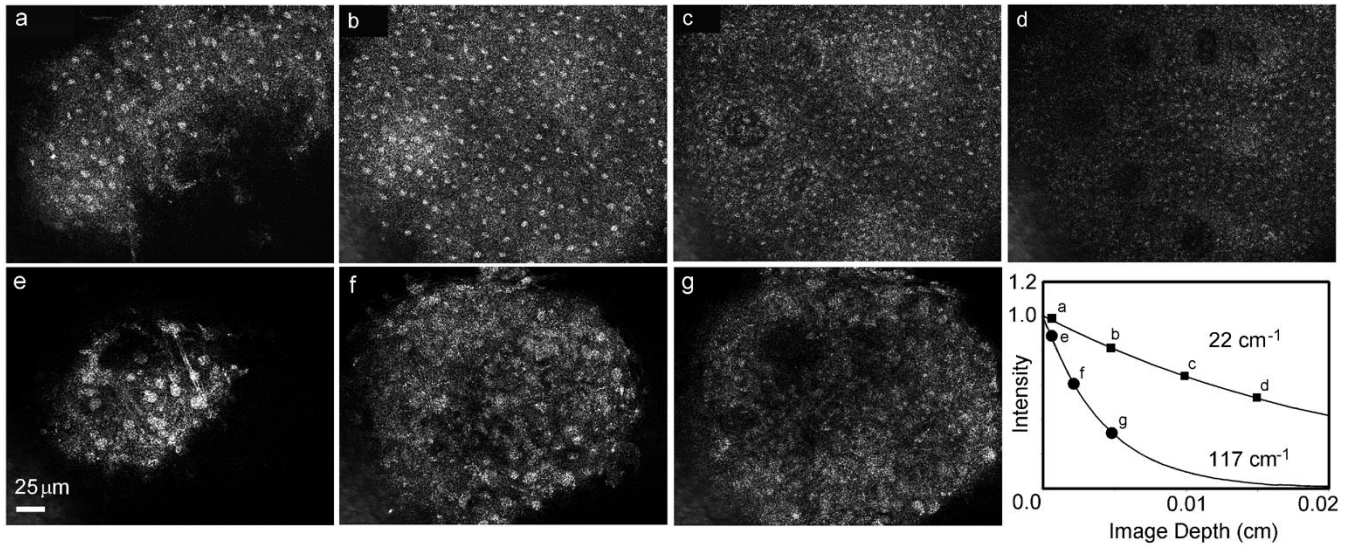


Fig. 1. Reflectance confocal images taken at various depths from a normal biopsy and a CIN 3 biopsy. Nuclei can be clearly visualized in images taken at varying depths within the epithelium of the normal biopsy at (a) 0 μm , (b) 50 μm , (c) 100 μm , and (d) 150 μm . Nuclei can only be visualized in the CIN 3 biopsy at image depths of: (e) 0 μm , (f) 25 μm , and (g) 50 μm . Attenuation of nuclear intensity is plotted for both biopsies with the estimated scattering coefficients illustrated.

coefficient [38]–[40]. With the reflected intensity measured using a confocal detection system from depth z , $I(z)$ can be expressed as

$$I(z) = I_0 e^{-\mu_t z} R(z) e^{-\mu_t z} = I_0 e^{-2\mu_t z} R(z) \quad (1)$$

where I_0 is the incident intensity, $R(z)$ is the depth dependent reflectivity, and μ_t is the attenuation coefficient, which is the sum of the absorption and scattering coefficients. Equation (1) assumes that excitation and reflected light travel parallel to the optical axis, which is equivalent to assuming a low numerical aperture. The equation can be used to analyze measurements of the intensity of reflected light measured as a function of depth to extract the attenuation coefficient of the epithelium, assuming that the reflectivity and the attenuation coefficient are not functions of depth within the epithelium. In the near infrared, where confocal measurements are frequently made, the absorption coefficient is significantly less than the scattering coefficient, so that this process can be used to estimate the epithelial tissue scattering coefficient [37].

The goal of the present study is to use (1) to analyze depth-dependent intensity measurements from confocal images of *ex vivo* cervical epithelium to estimate the scattering coefficient. In order to investigate the potential differences in scattering between normal and precancerous epithelium, measurements are made from both normal and precancerous tissue and compared with previous measurement of tissue scattering coefficients and numerical estimates of the scattering of normal and precancerous epithelial cells.

II. METHODS AND MATERIALS

A. Patients

Cervical biopsies were acquired from 25 patients at the colposcopy clinics of the University of Texas M.D. Anderson Cancer Center, Herman Hospital, and Lyndon Baines Johnson

Hospital, Houston, TX. The patients were referred to these clinics for suspected dysplasia on the basis of an abnormal cervical cytology or for removal of cervical tissue using the loop electrical excision procedure (LEEP) due to a previous diagnosis of dysplasia. Informed consent was obtained from each patient, and the project was reviewed and approved by the Surveillance Committee at the University of Texas M.D. Anderson Cancer Center and the Institutional Review Board at the University of Texas at Austin. Samples were included in the analysis presented here if the diagnosis of the biopsy was normal squamous epithelium or cervical intraepithelial neoplasia 3 (CIN 3) which indicates that dysplastic cells have been discovered in the upper one-third of the epithelium.

B. Specimens

Two uterine cervix biopsies were acquired from each patient. One of the biopsies was taken from a colposcopically normal area and the other was taken from a colposcopically abnormal area of the cervix and immediately placed in growth media (DMEM, no phenol red). Colposcopic impression (normal/abnormal) was recorded for each biopsy. The biopsies were approximately 3 mm wide by 4 mm long by 2 mm thick. Reflectance confocal images were taken of the biopsies within 6 h of excision.

C. Confocal Imaging

Reflectance confocal images were obtained from each biopsy using an epi-illumination laser scanning confocal microscope described in [15]. The illumination source was a continuous wave diode laser operating at 810 nm. Images were acquired with a 25X 0.8 NA water immersion objective (Plan-Neofluar multi-immersion, Zeiss). The confocal system operates at a dimensionless pinhole radius of 2.5 to provide maximum optical sectioning for obtaining cellular detail. The measured lateral and axial resolution of the system are 0.8 and 2–3 μm , respectively.

Immediately prior to imaging, biopsies were removed from growth medium and rinsed with PBS. A 6% solution of acetic acid was then added to each sample and image frames were acquired at various epithelial depths up to the working distance of the microscope, 250 μm . Images were acquired with the image plane parallel to the tissue surface. Images were digitized using a video frame grabber card and displayed at 7.5 frames per second on a computer monitor. Individual bitmap image files were saved from the frame grabber's video buffer. All specimens were then submitted for routine histologic examination using hemotoxylin and eosin stain. Sections were examined by an experienced board certified gynecologic pathologist (AM).

D. Image Processing

Images from each biopsy were processed to extract the reflected intensity from cell nuclei as a function of depth beneath the tissue surface. At each depth that an image was obtained, the mean gray scale intensity was measured from all visible nuclei. The mean reflected intensity was plotted as a function of depth from each biopsy. These data were fit to (1) by minimizing the mean square error between the data and the fit with the scattering coefficient as the only variable parameter.

III. RESULTS

Images were available from 19 biopsies from ten patients diagnosed as normal or CIN 3; 15 of these were diagnosed as squamous normal tissue and four were diagnosed as CIN 3. Fig. 1 shows a series of images taken at varying image depths from a histologically normal biopsy and a biopsy with CIN 3. Nuclei can be visualized in every image. The rate of intensity decrease is noticeably greater in the biopsy with CIN 3; nuclei can clearly be visualized at an image depth of 150 μm in the normal biopsy, but only to an image depth of 50 μm in the CIN 3 biopsy. The mean reflected intensity as a function of depth for these samples is illustrated in Fig. 1. Fits to (1) are also shown; the extracted scattering coefficient was 22 cm^{-1} for the normal biopsy and 117 cm^{-1} for the CIN 3 biopsy assuming that the absorption coefficient is small.

Fig. 2 illustrates fits to (1) for the 15 normal biopsies. In Fig. 2, the mean reflected intensity at the surface has been normalized to unity. The fits for all image sets had a mean correlation coefficient of greater than 0.95. The mean scattering coefficient was $22 \pm 5 \text{ cm}^{-1}$ with a minimum and maximum value of 14 and 30 cm^{-1} , respectively. Fig. 3 illustrates the fits to (1) for the four biopsies with CIN 3. The correlation coefficient is above 0.95 for the two biopsies with the highest decay rate and above 0.75 for the remaining two. The average scattering coefficient is $69 \pm 33 \text{ cm}^{-1}$; the minimum value is 44 cm^{-1} , and the maximum value is 117 cm^{-1} . Fig. 4 shows a scatter plot of the scattering coefficients for all specimens. Though the number of samples with CIN 3 is small, the average scattering coefficient is higher in the biopsies with CIN 3 than in the normal biopsies. The separation between normal and CIN 3 is clear. The results of a student's t-test indicate that the difference in mean scattering coefficients measured from the normal and CIN 3 biopsies is statistically significant ($P < 0.0001$).

Intensity Attenuation in Normal Biopsies

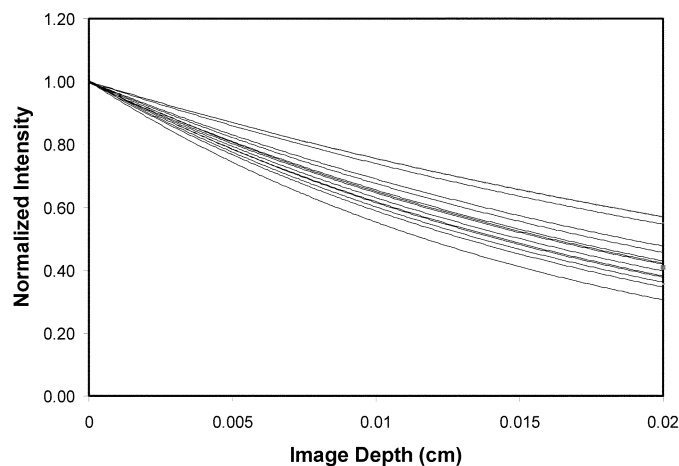


Fig. 2. Plot of the exponential fits from all normal biopsies; intensity at the tissue surface has been normalized to unity in each case. Mean scattering coefficient is $22 + / - 5 \text{ cm}^{-1}$.

Intensity Attenuation in Abnormal Biopsies

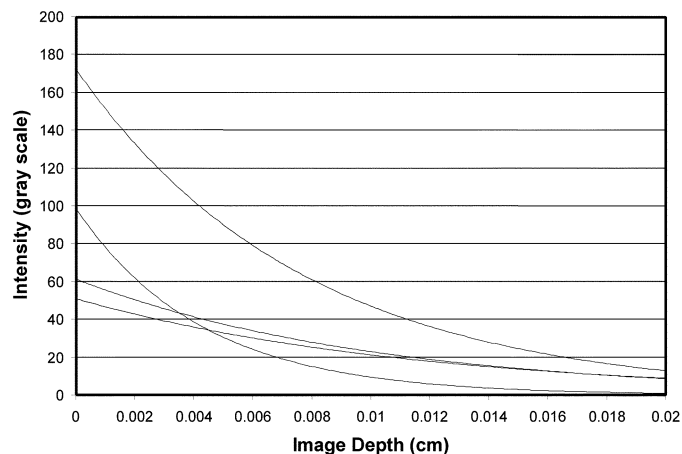


Fig. 3. Plot of the exponential fits from all CIN 3 biopsies. The mean scattering coefficient is $69 + / - 33 \text{ cm}^{-1}$.

IV. DISCUSSION

Table I presents scattering coefficients measured here for normal and precancerous cervix at 810 nm and compares these values to those reported in the literature for cervical, bladder, skin, and other epithelial tissues. Mourant studied the wavelength dependence of tissue scattering and noted that the scattering coefficient decreases with wavelength as $1/\lambda^{1.1}$ [45]. Table I calculates the scattering coefficient at 810 nm for other tissues assuming this relationship. The scattering coefficients measured here are significantly lower for normal cervical epithelium (22 cm^{-1}) than those previously reported for bulk scattering in cervical tissue (66–150 cm^{-1} at 800 nm) and in other epithelial tissues 53–370 (cm^{-1}). To our knowledge, they are also lower than values reported for any other tissue type. This suggests a significant disparity between the scattering properties of the cervical epithelium and the underlying connective tissue which appears to produce most of

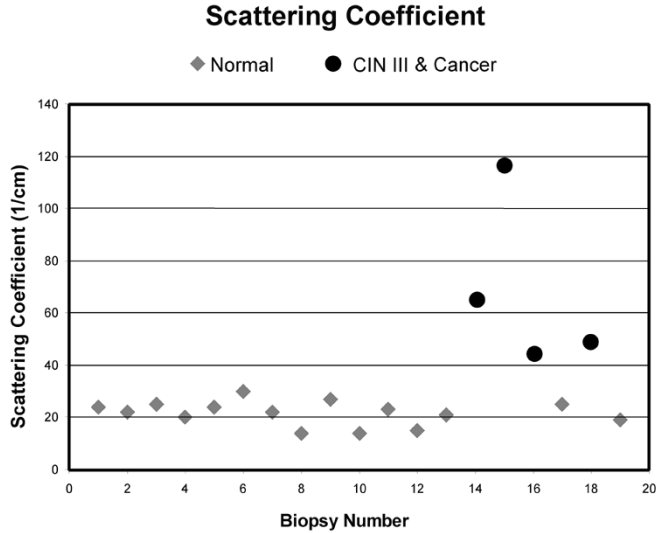


Fig. 4. Scatter plot of the scattering coefficients for all biopsies. Difference in the mean scattering coefficients of normal biopsies and CIN 3 biopsies are statistically significant ($P < 0.0001$).

TABLE I
REPORTED SCATTERING COEFFICIENT VALUES FOR EPITHELIAL TISSUES

Reported Scattering Coefficients				
Organ Site	Reference	Wavelength Measured (nm)	μ_s (cm^{-1})	μ_s (cm^{-1}) @ 810 nm
Cervix (normal)	This Paper	810	22	22
Cervix (precancerous)	This Paper	810	69	69
Cervix	36	800	66-100	65-99
Uterus	30	635	394	301
Breast	41	810	150	150
Breast	42	1100	100-500	140-700
Bronchial tissue epithelium	37	700	200	170
Esophagus	35	630	70	53
Skin	30	633	187	143
Skin	43	810	370	370
Skin	44	1000	160	127

the scattering. Further evidence for this conclusion can be made by considering the scattering properties of connective tissue alone. The scattering coefficient has recently been extracted from RAFT cultures composed of rat tail collagen and human fibroblasts [46] using second harmonic generation imaging. A value of 137 cm^{-1} was measured. The agreement between the values for bulk cervical tissue and the RAFT culture suggests that a majority of the scattering in bulk tissue is caused by the underlying connective tissue.

The scattering coefficients reported here for precancerous tissue (69 cm^{-1}) are significantly higher than the measurements for normal epithelium (22 cm^{-1}). We suspect that the increased scattering in the dysplastic tissue is due to changes in nuclear morphology. Quantitative measurements of the nuclear size and nuclear density from the same confocal image sets indicate that both are increased in CIN 3 [15]. Changes in chromatin optical density and texture within the nucleus are also suspected to cause increased scattering in the dysplastic tissue. We compared the scattering coefficient values measured here with values calculated using our finite-difference time-domain (FDTD) algorithm described in [47]. Estimating the volume fraction of nuclei and average nuclear size from the confocal images and

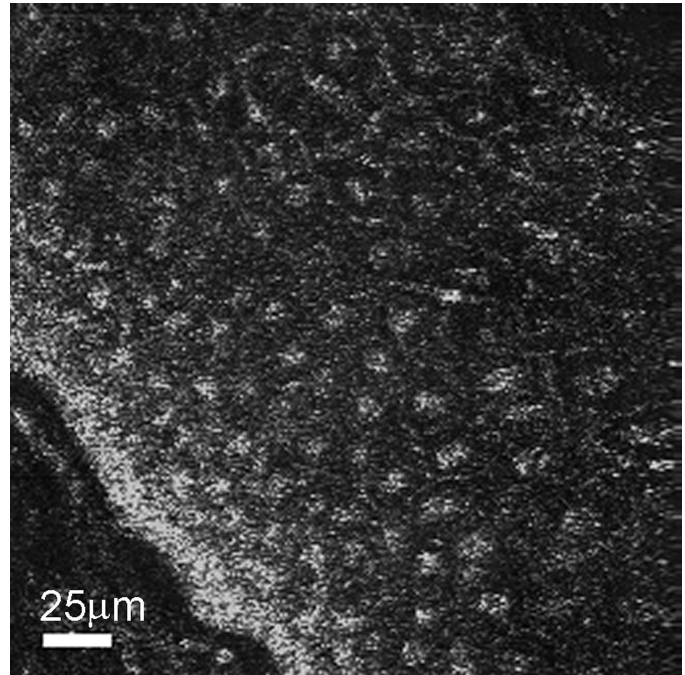


Fig. 5. Confocal image of *ex vivo* transverse sectioned biopsy. Depth-dependent reflectance is apparent with brighter nuclei near the basement membrane at the lower left corner of the image compared to those near the biopsy surface at the upper right corner of the image.

using the scattering cross section obtained using our FDTD algorithm, we predict the scattering coefficient for the normal and dysplastic tissue to be 13 and 142 cm^{-1} , respectively, at 810 nm . These values compare reasonably well with the values extracted from the confocal images (22 and 69 cm^{-1}) and give further evidence of increased scattering in the abnormal tissue.

A limitation of the current study is that confocal images were acquired from only three to five different depths. Increasing the number of images in each image stack would provide further evidence to indicate whether the signal decay is truly exponential. In the exponential fitting performed here, it has been assumed that the reflectance of the nuclei is constant as a function of depth within the epithelium. Confocal reflectance images taken of a transverse section of fresh cervical tissue (Fig. 5) indicate that this may not be the case. In Fig. 5, it is evident that the nuclei deep within the tissue, near the basement membrane, reflect more light than those near the top of the epithelium. This is consistent with FDTD models of the scattering cross section of superficial and basal epithelial cells where it has been hypothesized that increased nuclear optical density and increased refractive index heterogeneities within the nuclei cause increased backscattering from the basal cells [47]. The confocal image of the transverse section provides a direct measure of $R(z)$, the reflectivity as a function of depth. In future work, this can be used to improve estimation of the depth dependent scattering coefficient. In addition, the scattering coefficients estimated here are not corrected for the finite NA of the detection system. The maximum incident angle is 37° with this system, so this may overestimate the scattering coefficient by as much as $1/\cos(37^\circ) = 125\%$. Finally, we assume that the absorption coefficient is negligible compared

to the scattering coefficient at 810 nm. This is likely reasonable as the absorption coefficient of amelanotic epithelial tissues, including the cervix, has been reported with measurements below 1 cm^{-1} [30], [37].

The results presented here have important implications for computational tissue modeling of epithelial tissue fluorescence and reflectance and for optical probe design for *in vivo* data and image acquisition. The disparity of scattering between the epithelium and stroma suggests that single-layer tissue models that assume tissue is homogeneous are not well suited to describe propagation of light through epithelial tissue. The low scattering coefficient of the epithelium implies deeper light penetration within tissue, likely below the basement membrane and into the stroma.

Pfefer [27], Pogue [28], and Ramanujam [29] have shown that parameters such as the fiber diameter, source-to-collection fiber separation, and probe-to-tissue surface distance all affect the mean path length and collection efficiency of optical probes and imaging systems. Pogue demonstrated a fiber optic probe where the signal intensity is not significantly affected by the medium's absorption and scattering coefficients, but depends only on the properties of the fluorophores. This design was based on Monte Carlo simulations of a homogeneous medium with a scattering coefficient of 100 cm^{-1} , well above what we find for the epithelial layer of cervical tissue. Ramanujam presented a concept to locate the depth of a target layer of precancerous tissue between a normal epithelial layer and a stromal layer. This method was based on exciting and recording the fluorescence through apertures of variable diameter. Assuming the same scattering coefficient for all three layers (100 cm^{-1}), she showed that the variable aperture imaging method could be used to determine the depth dependence of the fluorescence contrast provided by the precancerous epithelium. Again, these calculations assume a much larger epithelial scattering coefficient than measured here. Pfefer presented an extensive Monte Carlo modeling study to investigate design parameters of the fiber optic probes. Assuming that the optical properties are homogeneous, with scattering coefficients ranging from $70\text{--}140 \text{ cm}^{-1}$, he studied the impact of tissue optical properties on fluorescence spectra. For example, Pfefer found an increase in axial selectivity with decreasing fiber radius. The conclusions of all these studies may not be applicable to cervical tissue, since the cervix has a layered structure and a lower scattering coefficient for the epithelial layer than used in these calculations. The design of fiber optic probes and imaging systems is critical to optimizing diagnostic information, and further work using the appropriate scattering coefficients is needed.

The lower scattering values also suggest improved imaging depths for many imaging modalities. The fundamental limit for reflectance based imaging within tissue is high scattering. A change in the scattering coefficient from 100 (the often assumed value) to 22 cm^{-1} results in a twofold increase in imaging depth for epi-illumination imaging. This is particularly significant for imaging modalities such as confocal and two-photon microscopy that use longer wavelengths where scattering of light within tissue is the most significant source of signal loss.

Finally, the increase in epithelial scattering as tissue progresses from normal to precancerous itself may be a useful diagnostic tool. It is relatively easy to process the signals from imaging probes as well as probes which collect diffuse reflectance in order to detect an increase in scattering within the tissue. This measure could provide an additional feature in classification algorithms designed to distinguish normal from dysplastic tissue.

REFERENCES

- [1] J. R. Mourant, I. J. Bigio, J. Boyer, R. L. Conn, T. Johnson, and T. Shimada, "Spectroscopic diagnosis of bladder cancer with elastic light scattering," *Lasers Surg. Med.*, vol. 17, pp. 350–357, 1995.
- [2] Z. Ge, K. T. Schomacker, and N. S. Nishioka, "Identification of colonic dysplasia and neoplasia by diffuse reflectance spectroscopy and pattern recognition techniques," *Appl. Spectrosc.*, vol. 52, pp. 345–833, 1998.
- [3] F. Koenig, R. Larne, H. Enquist, F. J. McGovern, K. T. Schomacker, N. Kollias, and T. F. Deutsch, "Spectroscopic measurement of diffuse reflectance for enhanced detection of bladder carcinoma," *Urology*, vol. 51, pp. 342–345, 1998.
- [4] M. S. Feld, "Spectral pathology using reflected light," in *Biomedical Optical Spectroscopy Diagnostics*. Washington, DC: Optical Soc. Amer., 1998.
- [5] G. Zonios, L. T. Perelman, V. Backman, R. Manahoran, M. Fitzmaurice, J. Van Dam, and M. S. Feld, "Diffuse reflectance spectroscopy of human adenomatous colon polyps *in vivo*," *Appl. Opt.*, vol. 38, pp. 6628–6637, 1999.
- [6] I. J. Bigio and J. R. Mourant, "Ultraviolet and visible spectroscopies for tissue diagnostics: Fluorescence spectroscopy and elastic scattering spectroscopy," *Phys. Med. Biol.*, vol. 42, pp. 803–814, 1997.
- [7] R. Glasgold, M. Glasgold, H. Savage, J. Pinto, R. Alfano, and S. Schantz, "Tissue autofluorescence as an intermediate endpoint in NMBA-induced esophageal carcinogenesis," *Cancer Lett.*, vol. 82, pp. 33–41, Jul. 1994.
- [8] R. Alfano, A. Pradhan, G. Tang, and S. Wahl, "Optical spectroscopic diagnosis of cancer and normal breast tissues," *J. Opt. Soc. Amer. B.*, vol. 6, pp. 1015–1023, 1989.
- [9] R. Richards-Kortum and E. Sevick-Muraca, "Quantitative optical spectroscopy for tissue diagnosis," *Annu. Rev. Phys. Chem.*, vol. 47, pp. 555–606, 1996.
- [10] I. Georgakoudi, B. C. Jacobson, J. Van Dam, V. Backman, M. B. Wallace, M. G. Muller, Q. Zhang, K. Badizadegan, D. Sun, G. A. Thomas, L. T. Perelman, and M. S. Feld, "Fluorescence, reflectance, and light-scattering spectroscopy for evaluating dysplasia in patients with Barrett's esophagus," *Gastroenterology*, vol. 120, no. 7, pp. 1620–1629, June 2001.
- [11] J. D. Pitts, R. D. Sloboda, K. H. Dragnev, E. Dmitrovsky, and M. A. Mycek, "Autofluorescence characteristics of immortalized and carcinogen-transformed human bronchial epithelial cells," *J. Biomed. Opt.*, vol. 6, pp. 31–40, Jan. 2001.
- [12] F. Koenig, F. J. McGovern, A. F. Althausen, T. F. Deutsch, and K. T. Schomacker, "Laser induced autofluorescence diagnosis of bladder cancer," *J. Urol.*, vol. 156, pp. 1597–1601, Nov. 1996.
- [13] Z. Huang, H. Zeng, I. Havzavi, D. McLean, and H. Lui, "Rapid near-infrared Raman spectroscopy system for real-time *in vivo* skin measurements," *Opt. Lett.*, vol. 26, pp. 1782–1784, 2001.
- [14] A. Mahadevan-Jansen and R. Richards-Kortum, "Raman spectroscopy for the detection of cancers and precancers," *J. Biomed. Opt.*, vol. 1, pp. 31–70, 1996.
- [15] T. Collier, A. Lacy, A. Malpica, M. Follen, and R. Richards-Kortum, "Near real time confocal microscopy of amelanotic tissue: Detection of dysplasia in *ex vivo* cervical tissue," *Acad. Radiol.*, vol. 9, pp. 504–512, 2002.
- [16] M. Rajadhyaksha, G. Menaker, T. Flotte, P. J. Dwyer, and S. Gonzalez, "Confocal examination of nonmelanoma cancers in thick skin excisions to potentially guide mohs micrographic surgery without frozen histopathology," *J. Investigative Dermatol.*, vol. 117, pp. 1137–1143, 2001.
- [17] J. Busam, K. Hester, C. Charles, D. Sachs, C. Antonescu, S. Gonzalez, and A. Halpern, "Detection of clinically amelanotic malignant melanoma and assessment of its margins by *in vivo* confocal scanning laser microscopy," *Acad. Dermatol.*, vol. 137, pp. 923–929, 2001.

- [18] M. E. Brezinski, G. J. Tearney, B. E. Bouma, J. A. Izatt, M. R. Hee, E. A. Swanson, J. F. Southern, and J. G. Fujimoto, "Optical coherence tomography for optical biopsy," *Circulation*, pp. 1206–1213, 1996.
- [19] F. I. Feldchtein, V. M. Gelikonov, G. V. Gelikonov, R. V. Kuranov, N. D. Gladkova, A. M. Sergeev, N. M. Shakhova, I. A. Kuznetsova, A. M. Denisenko, and O. S. Streltsova, "Design and performance of an endoscopic OCT system for *in vivo* studies of human mucosa," in *Proc. Conf. Lasers Electro-Opt.*, San Francisco, CA, 1998.
- [20] R. Drezek, M. Guillaud, T. Collier, I. Boiko, A. Malpica, C. Macaulay, M. Follen, and R. Richards-Kortum, "Light scattering from cervical cells throughout neoplastic progression: Influence of nuclear morphology, DNA content, and chromatin texture," *Biophys. J.*, 2001.
- [21] K. Sokolov, R. Drezek, K. Gossage, and R. Richards-Kortum, "Reflectance spectroscopy with polarized light: Is it sensitive to cellular and nuclear morphology?," *Opt. Express*, vol. 5, pp. 302–317, 1999.
- [22] W. K. Hong and M. B. Sporn, "Recent advances in chemoprevention of cancer," *Science*, vol. 278, pp. 1073–1077, Nov. 1997.
- [23] I. Georgakoudi, E. E. Sheets, M. G. Muller, V. Backman, C. P. Crum, K. Badizadegan, R. R. Dasari, and M. S. Feld, "Trimodal spectroscopy for the detection and characterization of cervical precancers *in vivo*," *Amer. J. Obstetrics Gynecol.*, vol. 186, no. 3, pp. 374–382, Mar. 2002.
- [24] I. Pavlova, K. Sokolov, R. Drezek, A. Malpica, M. Follen, and R. Richards-Kortum, "Microanatomical and biochemical origins of normal and precancerous cervical autofluorescence using laser scanning fluorescence confocal microscopy," *Photochem. Photobiol.*
- [25] R. Drezek, C. Brookner, I. Pavlova, I. Boiko, A. Malpica, R. Lotan, M. Follen, and R. Richards-Kortum, "Autofluorescence microscopy of fresh cervical-tissue sections reveals alterations in tissue biochemistry with dysplasia," *Photochem. Photobiol.*, vol. 73, no. 6, pp. 636–641, June 2001.
- [26] R. J. Hunter, M. S. Patterson, T. J. Farrell, and J. E. Hayward, "Hemoglobin oxygenation of a two-layer tissue-simulating phantom from time-resolved reflectance: Effect of top layer thickness," *Phys. Med. Biol.*, vol. 47, no. 2, pp. 193–208, Jan. 21, 2002.
- [27] T. J. Pfefer, K. T. Schomacker, M. N. Ediger, and N. S. Nishioka, "Multiple-fiber probe design for fluorescence spectroscopy in tissue," *Appl. Opt.*, vol. 41, pp. 4712–4721, Aug. 2002.
- [28] B. W. Pogue and G. Burke, "Fiber-optic bundle design for quantitative fluorescence measurements from tissue," *Appl. Opt.*, vol. 31, pp. 7429–7436, Nov. 1998.
- [29] L. Quan and N. Ramanujam, "Relationship between depth of a target in a turbid medium and fluorescence measured by a variable aperture method," *Opt. Express*, vol. 27, pp. 104–106, Jan. 2002.
- [30] W. Cheong, S. Prahl, and A. Welch, "A review of the optical properties of biological tissues," *IEEE J. Quantum Electron.*, vol. 26, pp. 2166–2185, Dec. 1990.
- [31] J. W. Pickering, S. A. Prahl, N. van Wierington, J. F. Beek, H. J. C. M. Sterenborg, and M. J. C. van Gemert, "Double-integrating-sphere system for measuring the optical properties of tissue," *Appl. Opt.*, vol. 33, pp. 399–410, 1993.
- [32] S. A. Prahl, M. J. C. van Gemert, and A. J. Welch, "Determining the optical properties of turbid media by using the adding-doubling method," *Appl. Opt.*, vol. 32, pp. 559–568, 1993.
- [33] T. Foster and E. Hull, "Optical tomography and spectroscopy of tissue: Theory, instrumentation, model and human studies II," in *Proc. SPIE-Int. Soc. Opt Eng.*, vol. 2979, 1997, p. 337.
- [34] S. Lin, L. Wang, S. Jacques, and F. Tittel, "Measurement of tissue optical properties using oblique incidence optical fiber reflectometry," *Appl. Opt.*, vol. 36, pp. 136–143, 1997.
- [35] R. Bays, G. Wagnieres, D. Robert, D. Braichotte, J. Savory, P. Monnier, and H. van den Bergh, "Clinical determination of tissue optical properties by endoscopic spatially resolved reflectometry," *Appl. Opt.*, vol. 35, pp. 1756–1766, Apr. 1996.
- [36] R. Hornung, T. H. Pham, K. A. Keefel, M. W. Berns, Y. Tadir, and B. J. Tromberg, "Quantitative near-infrared spectroscopy of cervical dysplasia *in vivo*," *Human Reproduction*, vol. 14, pp. 2908–2916, Nov. 1999.
- [37] J. Qu, C. MacAuley, S. Lam, and B. Palcic, "Optical properties of normal and carcinomatous bronchial tissue," *Appl. Opt.*, vol. 33, pp. 7397–7405, Nov. 1994.
- [38] C. Smithpeter, A. Dunn, A. Welch, and R. Richards-Kortum, "Penetration depth limits of *in vivo* confocal reflectance imaging," *Appl. Opt.*, vol. 37, pp. 2749–2754, 1998.
- [39] M. Kempe, W. Rudolph, and E. Welsch, "Comparative study of confocal and heterodyne microscopy for imaging through scattering media," *J. Opt. Soc. Amer.*, vol. 13, pp. 46–52, 1996.
- [40] J. Schmitt, A. Knüttel, and M. Yadlowsky, "Confocal microscopy in turbid media," *J. Opt. Soc. Amer.*, vol. 11, pp. 2226–2235, 1994.
- [41] J. Key, E. R. Davies, R. C. Jackson, and P. N. Wells, "Optical attenuation characteristics of breast tissues at visible and near-infrared wavelengths," *Phys. Med. Biol.*, vol. 36, pp. 579–590, May 1991.
- [42] V. G. Peters, D. R. Wyman, M. S. Patterson, and G. L. Frank, "Optical properties of normal and diseased human breast tissues in the visible and near infrared," *Phys. Med. Biol.*, vol. 35, pp. 1317–1334, Sept. 1990.
- [43] C. R. Simpson, M. Kohl, M. Essenpreis, and M. Cope, "Near-infrared optical properties of *ex vivo* human skin and subcutaneous tissues measured using the Monte Carlo inversion technique," *Phys. Med. Biol.*, vol. 43, pp. 2465–2478, Sept. 1998.
- [44] T. L. Troy and S. N. Thennadil, "Optical properties of human skin in the near infrared wavelength range of 1000 to 2200 nm," *J. Biomed. Opt.*, vol. 6, pp. 167–176, Apr. 2001.
- [45] J. R. Mourant, T. Fuselier, J. Boyer, T. M. Johnson, and I. J. Bigio, "Predictions and measurements of scattering and absorption over broad wavelength ranges in tissue phantoms," *Appl. Opt.*, vol. 36, pp. 949–957, Feb. 1997.
- [46] A. Zoumi, A. Yeh, and B. J. Tromberg, "Imaging cells and extracellular matrix *in vivo* by using second-harmonic generation and two-photon excited fluorescence," *Proc. Nat. Acad. Amer.*, vol. 99, pp. 11 014–11 019, Aug. 2002.
- [47] D. Arifler, M. Guillaud, A. Carraro, A. Malpica, M. Follen, and R. Richards-Kortum, "Light scattering from normal and dysplastic cervical cells at different epithelial depths: Finite-difference time-domain modeling with a perfectly matched layer boundary condition," *J. Biomed. Opt.*, vol. 38, submitted for publication.



Tom Collier received the B.S. in architecture from the University of Texas at Austin, in 1987. He worked as a registered architect until reentering The University of Texas where he received the M.S. degree in electrical engineering in 2000. He is currently pursuing the Ph.D. degree in electrical engineering at the same university.

Dizem Arifler received the B.S. degree in physics and the M.S. degree in biomedical engineering from The University of Texas at Austin, in 2000 and 2002, respectively. She is currently pursuing the Ph.D. degree in biomedical engineering at the same university.

Her research interests include numerical modeling of light scattering from cells and model-based analysis of reflectance spectroscopy.



Anais Malpica received the M.D. degree from the Universidad Central de Venezuela, Caracas, in 1984.

She trained in anatomic and clinical pathology at Boston University, Boston, MA, and Baylor College of Medicine between 1987 and 1992. After that, she completed a fellowship in surgical pathology at The University of Texas M. D. Anderson Cancer Center, Houston, TX, in 1993. She is currently an Associate Professor of Pathology at the University of Texas M. D. Anderson Cancer Center. She has collaborated on several projects involving the use of optical spectroscopy for the detection of preinvasive epithelial cervical lesions. Her research interests include the analysis of clinicopathologic features of different entities in the gynecological tract and the study of cervical preinvasive lesions.



Michele Follen received the B.A. degree from the University of Michigan, Ann Arbor, in 1975, the M.D. degree from the University of Michigan Medical School in 1980, and the M.S. degree in clinical research design and the Ph.D. degree in epidemiology from the University of Michigan, Ann Arbor, in 1989 and 2000, respectively.

She is a Professor of Gynecologic Oncology and the Director of the Biomedical Engineering Center at the University of Texas M. D. Anderson Cancer Center. She is the Director of the Colposcopy Clinic at the M. D. Anderson Cancer Center and the Division Director of Gynecologic Oncology at The University of Texas Health Science Center-Lyndon Baines Johnson Hospital, Houston, TX. She is also a Professor in Biomedical Engineering at the University of Texas at Austin. Her research interests include the use of optical spectroscopy and imaging for detection of cervical precancer and treatment of preinvasive cervical neoplasia with chemo-preventive agents.



Rebecca Richards-Kortum received the B.S. degree in physics and mathematics from the University of Nebraska, Lincoln, in 1985, and the M.S. degree in physics and the Ph.D. degree in medical physics at Massachusetts Institute of Technology, Cambridge, in 1987 and 1990, respectively.

She began her academic career at the University of Texas at Austin in the Electrical and Computer Engineering Department as an Assistant Professor in 1990. She currently holds the Robert M. And Prudie Leibrock Endowed Professor in Engineering and is the Associate Chair for Research in the newly formed Biomedical Engineering Department at The University of Texas at Austin. She is also a Distinguished Teaching Professor at the university. She directs an Integrative Graduate Education and Research Training Grant in Optical Biomolecular Engineering. Her research focuses on the application of optical imaging and spectroscopy for detection of precancer and other diseases.

Dr. Richards-Kortum's awards include the Presidential Young Investigator, National Science Foundation (1991 and 1992), Presidential Faculty Fellow, Becton Dickinson Career Achievement Award, Association for the Advancement of Medical Instrumentation (1992), Outstanding Engineering Teaching by an Assistant Professor Award, College of Engineering, The University of Texas at Austin (1994), and Y. C. Fung Young Investigator Award, Bioengineering Division, American Society of Mechanical Engineers (1999). She is a member of the American Association for the Advancement of Science, American Association for Cancer Research, American Institute for Medical and Biological Engineering, American Society for Engineering Education, American Society for Laser Medicine and Surgery, American Society for Photobiology, Optical Society of America, and Society for Applied Spectroscopy.